Primordial Disk Evolution

A timescale analysis

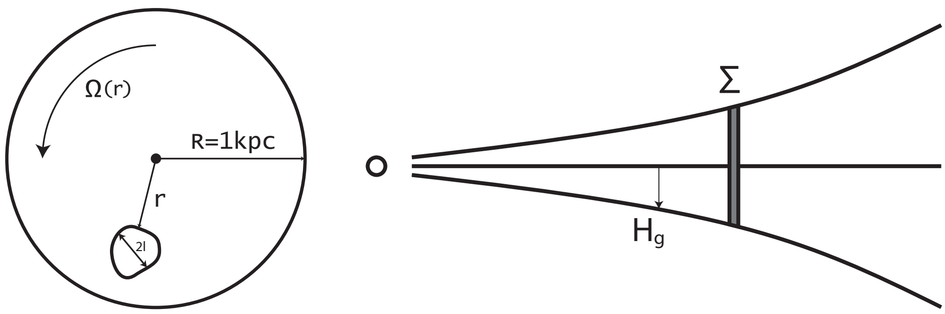

Ellen Schallig

Bachelor Thesis Astronomy

16 June 2012

Primordial Disk Evolution

Summary

To study the formation of structure in primordial disks, we developed a model of a disk consisting of 75% H and 25% He by mass, that takes into account gravitational influences, cooling, shearing, photodissociation and supernova events. Comparing the timescales of the different processes, we found that the disk can form objects with $M_J = 10^4 - 10^6 \mathrm{M}_\odot$ for Lyman-α cooling dominated regions and $M_J =$ few $10^2 - 10^3$ $\mathrm{M}_\odot$ for H_2 dominated regions. Most of the disk however, from about 200 pc outwards, will not form objects. The photodissociating UV background is sufficient up to a few pc from a nearby star. H_2 cooling is most efficient in the central 50 pc. The shearing timescale and supernova timescale do not have a large influence on star formation.

Bachelor Thesis in Astronomy
Author: Ellen Schallig
Supervisor: prof. dr. Marco Spaans
Date: 16 June 2012

Kapteyn Astronomical Institute
Landleven 12
9747 AD Groningen
The Netherlands

Contents

Chapter 1

Background

In the very early universe, there were no galaxies or stars. It contained only hydrogen, helium, trace amounts of lithium, and large amounts of dark matter. All the heavier elements were synthesized in stars. This means that the processes in star formation today are not the same as the processes in the early universe, as star formation now depends strongly on the abundance of heavier elements.

Following Barkana and Loeb [2001] and Salvadori [2009], I will give an overview of the formation of the first structures below.

According to the standard model of cosmology, the ΛCDM (lambda cold dark matter) model, the present structure in the universe originated from small density fluctuations in the early universe. This theory is supported by the detection of small temperature fluctuations in the cosmic microwave background, $\frac{\Delta T_{\mathrm{CMB}}}{T_{\mathrm{CMB}}} = 10^{-5}$. This indicates that the universe started out extremely uniform and simple, see also figure 1.1.

The initial conditions for star formation in the early universe are fully specified by the power spectrum of the density fluctuations, the mean density of dark matter, the initial temperature and density of the cosmic gas, and the primordial composition. There are not yet metals or significant magnetic fields, and there is not yet feedback from luminous objects [Barkana and Loeb, 2001].

After the first stars and quasars formed, the universe gradually became ionized, and has remained so ever since. Calculations find that this reionization happened at a redshift z of $\sim 7 - 12$. It is unclear when and how exactly the first objects formed. Current telescopes cannot reach beyond $z \approx 8$ and have not been able to observe these first (Population III, metal-free) stars. One possible way to study these first objects is to examine the feedback effects they had on the current objects.

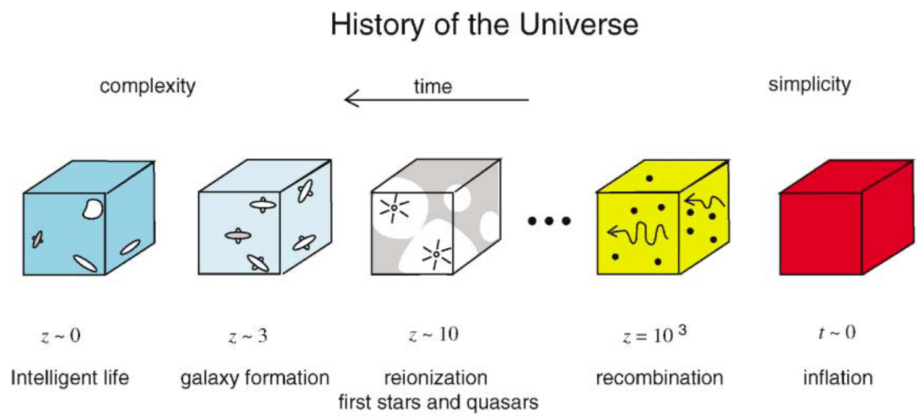

Figure 1.1: Milestones in the evolution of the universe, from simplicity to complexity, taken from Barkana and Loeb [2001].

The ΛCDM model predicts that as the dark matter clustered together, the baryonic matter fell into the subsequent potential wells. By cooling and condensation of the gas in the centers of these dark matter halos, protogalaxies were formed. These were the first building blocks of the universe.

1.1 Formation of dark matter halos

In the early universe the small density fluctuations (one in 10^5 as stated above) were not static. As long as those fluctuations are small, the mix of dark matter and baryons can be described by linear perturbation theory. The baryons can be seen as a collisional fluid and the dark matter as a collision-less one. This mix has an average mass density $\bar{\rho}$, and this density can be perturbed at any time and place by a dimensionless density perturbation $\delta(\mathbf{x}, t) = \frac{\bar{\rho}(t)}{\rho(\mathbf{x},t)} - 1$. The fluid is then described by the continuity and Euler equations as stated in paragraph 2.2 of Barkana and Loeb [2001]. For this problem there are in general two solutions: a growing mode and an oscillatory mode. For small perturbations ($\delta \ll 1$) the dominant solution grows with time and dominates the density evolution. This means that the density perturbation maintains its shape (in comoving coordinates). See Barkana and Loeb [2001] for a complete treatment of this problem. If the inward pressure in these perturbations is larger than the outward pressure, the structure collapses.

When the growing perturbations δ become of order unity, the full non-linear gravitational problem must be taken into account, as linear perturbation theory does not apply anymore. This happens with the dark matter at early epochs, as the growing dark matter perturbations interact only very weakly with the rest of the matter and the radiation field. The growth of these perturbations is not slowed unlike baryonic matter perturbations, which interact strongly with the radiation field.

The gravitational collapse of such a dark matter density perturbation can only be solved analytically in particular cases. The simplest case is the 'top-hat' spherical collapse: a spherically symmetric uniform overdensity inside a sphere of radius r. If the mass shell at this radius r is gravitationally bound, then the overdensity reaches a maximum radius of expansion and subsequently collapses to a point. If there is no exact spherical symmetry, the dark matter halo does not collapse to a point, but reaches virial equilibrium through the process of violent relaxation.

This, however, is not the complete story. At early times, most of the dark matter is in small (low-mass) halos, and the theory is that larger halos are formed by the merging of smaller halos. This is called hierarchical formation. Such a hierarchical growth puts constraints on the physics of halo formation, which Navarro et al. [1997] researched. They found that the density profile of the resulting halos is roughly universal. The abundance of these dark matter halos was modelled analytically by Press and Schechter in 1974. This simple model matches most of the numerical simulations. The halo abundance gives important clues towards the abundances of galaxies and galaxy clusters.

1.2 Gas infall in dark matter halos

The dark matter halos virialize at a time that baryonic matter cannot yet form gravitationally bound objects. Before the recombination era the photons and free electrons interact through Compton drag, which prevents the growth of density perturbations in the baryonic matter. After the decoupling and recombination, however, Compton drag is essentially zero and the perturbations can grow in the potential wells created by the dark matter halos.

As gravity becomes stronger, more matter is attracted. This matter will only fall to the center of the potential well if the associated energy is low enough. Dark matter cannot dissipate the extra energy to relax into these potential wells, but baryonic matter can, through cooling. As the gas cools through either atomic line cooling (the halo reaches $M = 10^8 - 10^9$ $\mathrm{M}_\odot$ and $T = 10^4$ K) or molecular hydrogen H_2 (the halo has $M = 10^5 - 10^6$ $\mathrm{M}_\odot$ and $T \lesssim 700$ K), the gas density in the center of the potential wells becomes much higher than the dark matter density. Therefore in the central few kpc of a halo dark matter can be ignored. Only in the outer regions it becomes the dominant source of gravity. See e.g. Guo et al. [2010] for more information on the relation between stellar mass and halo mass.

The minimum mass for the bound objects created by these perturbations is given by the Jeans mass M_J, which is the mass in a given volume that can collapse through its own gravity. This will only happen when the outward pressure is smaller than the inward (gravitational) pressure. The outward pressure consists mainly of thermal, magnetic, and turbulent pressure. However, Schleicher et al. [2010] state that the magnetic pressure is about $0.1 - 0.5$ times the thermal pressure. The largest contributors of turbulence are supernova events, but at these early times there are not enough to make a large impact on the total pressure. As the thermal pressure is much higher than magnetic or turbulent pressure, I have decided to ignore the latter two for this research.

For the temperature and thus thermal pressure to stay low during collapse, cooling has to be efficient. The cooling time has to be shorter than the time it takes for the matter to collapse under its own gravity: $t_{\mathrm{cool}} < t_{\mathrm{dyn}}$.

The Jeans mass at $z < 200$, when the gas temperature declines adiabatically through Hubble expansion, is given by [Salvadori, 2009]:

$$M_J = 3.08 \cdot 10^3 \left(\frac{\Omega_m h^2}{0.13}\right)^{-\frac{1}{2}} \left(\frac{\Omega_b h^2}{0.022}\right)^{-\frac{3}{5}} \left(\frac{1+z}{10}\right)^{\frac{3}{2}} M_\odot, \tag{1.1}$$

where Ω_m is the total matter density, Ω_b the baryon matter density, h the reduced Hubble constant and z the redshift.

Without cooling or heating processes the cooling rate is set by adiabatic cooling, namely, Hubble expansion. The associated timescale is:

$$t_{\mathrm{H}} = H(z)^{-1} = H_0^{-1}[\Omega_\Lambda + \Omega_m(1+z)^3]^{-\frac{1}{2}}, \tag{1.2}$$

where Ω_Λ is the dark energy density, and Ω_m and z are as above.

During the collapse, the density increases. The Jeans mass is density-dependent (see section 2.1), and will go down when the density goes up. Therefore, if the temperature stays low, the collapsing object can fragment into smaller objects, which each have to satisfy $t_{\mathrm{cool}} < t_{\mathrm{dyn}}$ to collapse further.

1.3 Feedback

As soon as the first stars form in the collapsed halos, the processes in these stars create so-called ‘feedback’ processes, which dramatically change the subsequent star formation. These processes are grouped together in three different classes: radiative, mechanical and chemical feedback.

1.3.1 Radiative feedback

As soon as the first stars form, they will produce UV radiation: radiation that excites molecular hydrogen, but cannot ionize it (11.2-13.6 eV, Lyman-Werner photons) and radiation that ionizes the hydrogen atom (>13.6 eV). When molecular hydrogen is excited, in about 15% of the cases the molecule dissociates through the Solomon process:

$$\begin{aligned} H_2 + \gamma &\rightarrow H_2^* \\ H_2^* &\rightarrow 2H + \gamma \end{aligned}$$

As molecular hydrogen is very important in the formation of the earliest stars, this acts as a negative feedback and reduces the star formation efficiency. When H_2 cooling is suppressed, the formation of massive objects is possible [Begelman et al., 2006].

At energies >13.6 eV, hydrogen atoms are ionized, and molecular hydrogen can form through the following process:

$$\begin{aligned} H + e^- &\rightarrow H^- + h\nu \\ H^- + H &\rightarrow H_2 + e^- \end{aligned}$$

This acts as positive feedback, as more H_2 means more cooling and thus more star formation. If halos contain miniquasars with photon energies extending to about 1 keV, then these X-rays balance the effects of the UV background [Haiman et al., 2000].

UV radiation cannot only ionize hydrogen atoms, but can also heat the gas and photo-evaporate it, thus destroying smaller halos. However, Dijkstra et al. [2004] have found that in the early universe this is not as effective as in the present-day universe, because (1) the amplitude of the ionizing background is lower, (2) the ionizing background turns on only after a substantial overdensity has formed inside the halo, (3) collisional cooling processes are more efficient at high redshift, and (4) the atoms can self-shield against the radiation.

1.3.2 Mechanical feedback

As the first stars are thought to be very massive, these end up mostly as supernovae. Supernova events (SNe) are so energetic that partial (or even total) removal of the gas from the galaxy is very likely, thereby reducing the star formation rate and the impact of the next generation of supernovae [Heger et al., 2002]. Whalen et al. [2008] found that a single SNe (with mass $15 - 40$ $M_\odot$) is sufficient to blow away all the gas from halos less massive than 10^7 $M_\odot$.

1.3.3 Chemical feedback

Star formation in the present-day universe relies heavily on the presence of metals and dust. Gas cooling can take place through collisions (dust and molecules) and line cooling (individual atoms). As stated before, cooling is necessary to keep star formation going. As supernovae deposit more metals and dust into the gas, cooling, and therefore star formation, becomes more efficient. In figure 1.2 the effect of these SNe is shown. In this simulation, done by Mori and Umemura [2006], stars more massive than 8 $M_\odot$ explode as type II supernovae with an explosion energy of 10^{51} erg, and eject synthesized heavy elements and dust. At first only the immediate neighborhood is enriched, and higher-metallicity bubbles exist in the otherwise primordial gas. As the shocks hit lower-density gas, the expansion of the hot, metal-rich bubbles is accelerated.

H_2 can also be made on the surfaces of dust grains. As soon as the dust-to-gas mass ratio is of the order of 10^{-3}, at $z \geq 3$, a positive feedback effect can occur for the abundance of H_2 molecules [Cazaux and Spaans, 2004]. This result depends strongly on the dust and gas temperatures.

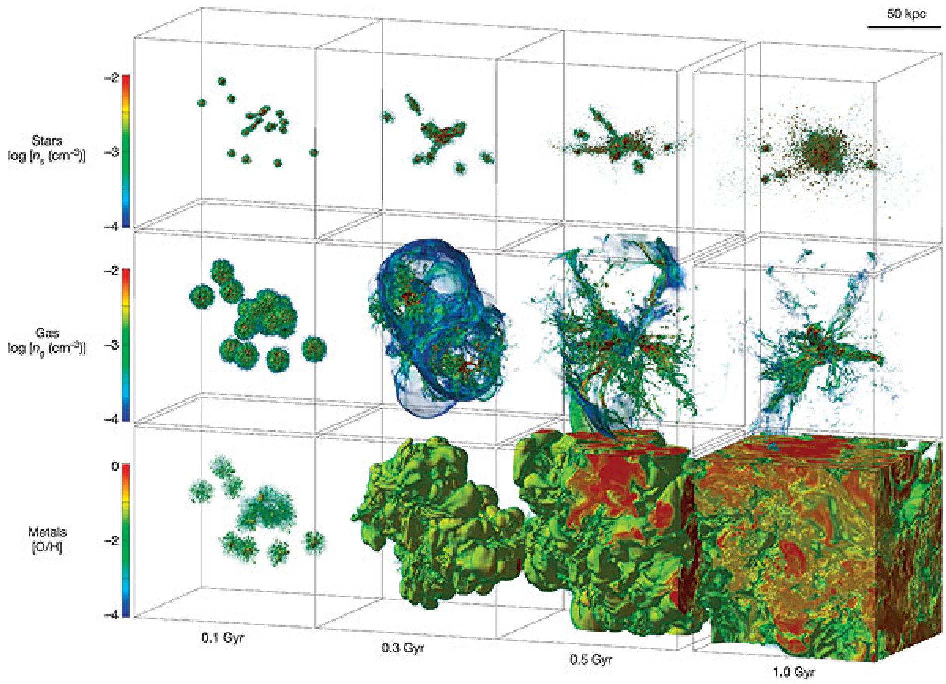

Figure 1.2: Spatial distribution of the stellar number density, gas number density and oxygen abundance of a protogalaxy with total mass 10^{10} $M_\odot$, taken from Mori and Umemura [2006].

1.4 This research

This research will focus on the star and black hole forming capacities of a disk at a redshift $10 < z < 15$. As matter settles into a potential well, due to conservation of angular momentum it will have to form a rotating disk. A seed black hole has already formed through singular collapse [Johnson et al., 2011]. The matter near the black hole will be attracted and rotate faster, flattening the disk. The lower limit for the redshift is chosen such that the disk is not yet a full-blown galaxy. However, it has had time to form the first stars, through which the metallicity is increased up to the limit needed for Salpeter-like star formation.

Chapter 2

Timescales

By looking at the timescales of different processes in a rotating gaseous disk, one is able to constrain the outcome of these dynamical processes. Important processes are gravitational collapse, the amount of cooling reached through H_2-cooling, HI- and HeII-Lyα-cooling, and viscous effects.

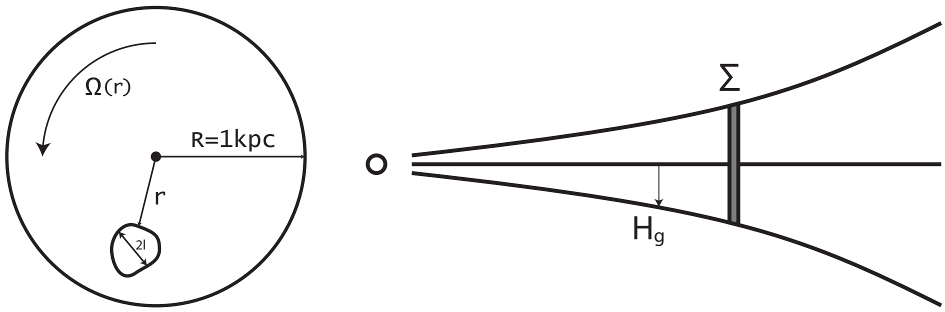

(a) seen from above

(b) seen from the side

Figure 2.1: Physical structure of the disk.

Our toy model disk has a total radius R, a scaleheight H_g, a surface density $\Sigma(r)$, and, following the relation Magorrian et al. [1998] found, a central mass roughly 0.006 times the total mass of the disk. Here the surface density is taken as the volume number density integrated over the total height of the disk. To find the speed $|v|$ of the gas at a certain radius, we must first calculate the enclosed mass at that radius:

$$M_c = \int_0^r m\Sigma(r)2\pi r \mathrm{d}r \tag{2.1}$$

where m is the mean mass of a primordial particle, with a primordial mixture of 75% H and 25% He by mass. We assume that $\Sigma(r) \propto \frac{1}{r^p}$. This means that M_c is proportional to r^{2-p}. For this disk we take the surface density to be 10^{23} cm^{-2} at 10 pc and 10^{21} cm^{-2} at 1 kpc, therefore for this case $p = 1$ and $M_c \propto r$. We can now see how this influences the speed of the gas, by balancing the gravitational and centripetal force:

$$\frac{GM_c m}{r^2} = \frac{mv^2}{r}. \tag{2.2}$$

G is the gravitational constant. From this we find that $|v| = \sqrt{\frac{GM_c}{r}}$, which is constant if there is no large central mass, and we also find the angular frequency $\Omega(r)$, as $\Omega = \frac{2\pi}{T} = \frac{|v|}{r}$. Thus

$$\Omega(r) = \sqrt{\frac{GM_c}{r^3}} \propto \frac{1}{r}. \tag{2.3}$$

If there is a large mass present in the center of the disk, for example a massive black hole, the enclosed mass will be dominated by this object. This means that the enclosed mass can be seen as a constant, and the speed and angular frequency of the gas change accordingly:

$$|v| = \sqrt{\frac{GM_c}{r}}, \qquad \Omega(r) = \sqrt{\frac{GM_c}{r^3}}, \qquad M_c \text{ is constant.} \tag{2.4}$$

This is called Keplerian motion.

2.1 Dynamical time

Information from one part of the disk to another will travel with the sound-speed c_s. This means that the gas pressure can react to changes in the cloud with that speed. If the pressure can react fast enough to density fluctuations, the gas is smoothed out, but if the density fluctuations have such a large wavelength that they are compressed faster by gravity than the pressure can damp them out, the gas will collapse. One can express this instability also as $4\pi G\rho_0 > k^2 c_s^2$, with ρ_0 the inital density and k the wavenumber. This means that there is a wavelength for which the pressure and gravity react equally fast: the Jeans length λ_J.

$$\lambda_J = \left(\frac{\pi c_s^2}{G\rho_0}\right)^{\frac{1}{2}}. \tag{2.5}$$

The total mass contained within this wavelength is $\sim \rho_0 \lambda_J^3$ and is called the Jeans mass [Clarke and Carswell, 2007, Frieswijk, 2008]:

$$M_J = \left(\frac{\pi c_s^2}{G}\right)^{\frac{3}{2}} \rho_0^{-\frac{1}{2}} \propto T^{\frac{3}{2}} \rho_0^{-\frac{1}{2}} \simeq 7.5 \left(\frac{T}{10\text{ K}}\right)^{\frac{3}{2}} \left(\frac{n}{10^4\text{ cm}^{-3}}\right)^{-\frac{1}{2}} M_\odot. \tag{2.6}$$

When $\lambda > \lambda_J$, or equivalently when the mass contained in this volume λ_J^3 is increased, the cloud can collapse. The time it takes to collapse under its own gravity (also known as self-gravity) is called the dynamical (or free-fall) time.

Using dimensional analysis on $4\pi G\rho_0 > k^2 c_s^2$, one can construct this corresponding timescale, because in cgs-units: $G = [\mathrm{cm}^3\ \mathrm{g}^{-1}\ \mathrm{s}^{-2}]$ and $\rho_0 = [\mathrm{g\ cm}^{-3}]$. The dynamical time in years then is:

$$t_{\mathrm{dyn}} \propto \frac{1}{\sqrt{G\rho_0}} \simeq 7.2 \cdot 10^5 \left(\frac{n}{10^4\ \mathrm{cm}^{-3}}\right)^{-\frac{1}{2}} [\mathrm{yr}]. \tag{2.7}$$

2.2 Cooling time

The temperature of the gas is important in the formation of structure. As we have seen before, the Jeans mass depends on the temperature as $T^{\frac{3}{2}}$. By cooling the gas, the Jeans mass is also lowered and fragmentation of the gas during collapse is a possibility.

In primordial gas cooling can take place through atomic hydrogen HI, molecular hydrogen H_2, hydrogen deuteride HD and ionic helium HeII. Of these, the only low-temperature coolants are H_2 and HD. These can bring the temperature down to a few hundred K. It is believed that the very first objects in the Universe were cooled primarily by H_2, which is effective at temperatures $T \gtrsim 200$ K and at gas number densities $n < 10^4\ \mathrm{cm}^{-3}$ [Glover and Abel, 2008]. HD can cool to lower temperatures at higher densities (up to $10^6\ \mathrm{cm}^{-3}$), thus bringing about lower characteristic masses, but it will only do so if enough is formed to cool efficiently. This does not happen when the virial temperature $T_{\mathrm{vir}} < 10^4$ K, but gas cooling from an initially ionized state will form enough HD to cool to very low temperatures [Glover and Abel, 2008]. This is possible because in hot gas that is cooled, more and more H_2 is formed, and more and more cooling takes place. Then only the reaction $H_2 + D^+ \rightarrow HD + H^+$ (exothermic) is possible, because its endotherm equivalent, $HD + H^+ \rightarrow H_2 + D^+$, only takes place above 462 K. Through this process enough HD can form to dominate the cooling.

At temperatures $10^4 \lesssim T \lesssim 10^5$ K cooling is primarily done through the HI-Lyman-α line [Haiman et al., 2000]. The radiative cooling rate is defined as $n^2\Lambda$ with units erg $\mathrm{cm}^{-3}\ \mathrm{s}^{-1}$. For Lyman-$\alpha$ cooling this rate is given by:

$$n^2\Lambda_{\mathrm{Ly}\alpha} \simeq 7.3 \cdot 10^{-19} n_{\mathrm{e}} n_{\mathrm{HI}} \exp(-118,400/T)\ \mathrm{erg\ cm}^{-3}\mathrm{s}^{-1},$$

with n_{e} and n_{HI} the electron and hydrogen atom number densities [Tielens, 2005]. In temperatures of 10^6 to 10^8 K cooling is due to free-free transitions [Latif et al., 2011]. In figure 2.2 the efficiency of the different cooling mechanisms is shown. For molecular hydrogen, atomic hydrogen, ionic helium

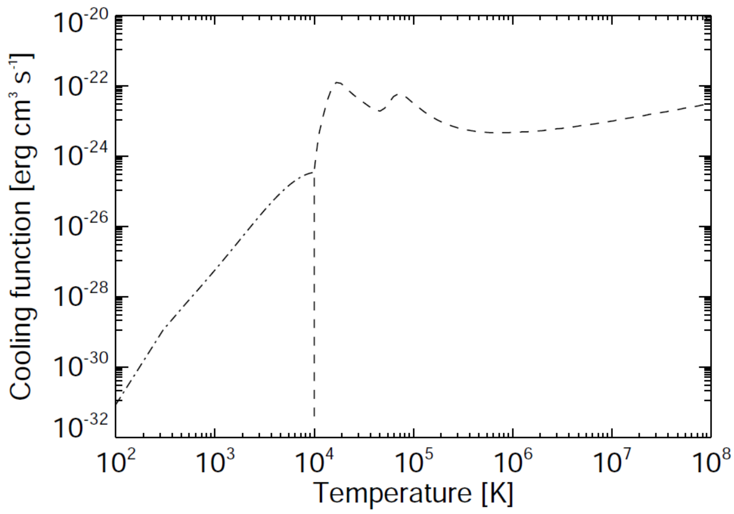

Figure 2.2: Cooling function for zero metallicity, taken from Latif et al. [2011]. The stripe-dotted line is cooling due to molecular hydrogen, the striped line shows the atomic cooling.

and free-free emission we can get values at certain temperatures from this graph:

$$\begin{aligned}
\Lambda_{\text{free-free}} &\simeq 10^{-24} \text{ erg cm}^3 \text{ s}^{-1} \text{ at } T = 10^6 \text{ K},\\
\Lambda_{\text{Ly}\alpha\text{HeII}} &\simeq 10^{-23} \text{ erg cm}^3 \text{ s}^{-1} \text{ at } T = 10^{4.8} \text{ K},\\
\Lambda_{\text{Ly}\alpha\text{HI}} &\simeq 10^{-22} \text{ erg cm}^3 \text{ s}^{-1} \text{ at } T = 10^4 \text{ K},\\
\Lambda_{\text{H}_2} &\simeq 10^{-28} \text{ erg cm}^3 \text{ s}^{-1} \text{ at } T = 700 \text{ K},\\
\Lambda_{\text{H}_2} &\simeq 10^{-30} \text{ erg cm}^3 \text{ s}^{-1} \text{ at } T = 200 \text{ K},\\
\Lambda_{\text{HD}} &\simeq 10^{-30} \text{ erg cm}^3 \text{ s}^{-1} \text{ at } T = 100 \text{ K}.
\end{aligned}$$

The hydrogen deuteride (HD) number at around 100 K is an estimate, taken from the fact that HD-cooling takes over from H_2 for temperatures lower than 200 K.

The radiative cooling function Λ has units erg cm^3 s^{-1}. To get rid of the energy and volume components, we multiply by n and divide by kT, the number density and characteristic energy. We then get the following timescale:

$$t_{\text{cool}} = \frac{kT}{n\Lambda}. \tag{2.8}$$

The cooling timescale is dependent on the dominant cooling mechanism. H_2 and HD are only abundant enough to cool the gas in places with $n \geqslant$

dominant cooling	Λ [erg cm^3 s^{-1}]	T [K]	n [cm^{-3}]	t_{cool} [yr]
free-free emission	10^{-24}	10^6	10^{-1}	$4 \cdot 10^7$
HeII Lyman-α	10^{-23}	$10^{4.8}$	10^0	$3 \cdot 10^4$
HI Lyman-α	10^{-22}	10^4	10^0	$5 \cdot 10^2$
H_2 (700 K)	10^{-28}	700	10^3	$3 \cdot 10^4$
H_2 (200 K)	10^{-30}	200	10^3	$9 \cdot 10^5$
HD	10^{-30}	100	10^3	$4 \cdot 10^5$

Table 2.1: Cooling times for the different cooling mechanisms, taking into account the necessary temperatures and number densities for those mechanisms to be dominant.

10^3 cm^{-3}. Lyman-α is most effective when the temperature is $10^4 - 10^6$ K and free-free emission is the dominant cooling mechanism when $T > 10^6$ K [Latif et al., 2011]. Now we can calculate the corresponding cooling times, arranged in table 2.1.

2.3 Photodissociation time

In a cloud consisting of primordial gas, at low temperatures the only way for the gas to cool efficiently is the collisional excitation of H_2 molecules: hydrogen atoms collide with the molecules and excite them. When the molecule falls back to the ground state, the photon emitted is of such energy that it is not again absorbed by the gas, and thus its energy is lost. In other words, the H_2 cooling lines are mostly optically thin. H_2 molecules are very susceptible to photon absorption in the 912-1108 Å range (Lyman-Werner photons). These photons are produced by young stars in the neighbourhood and form the so-called 'UV background' G_0 which is usually expressed in terms of the equivalent one-dimensional average interstellar radiation field flux of $1.6 \cdot 10^{-3}$ erg cm^{-2} s^{-1} [Tielens, 2005]. In the Milky Way, $G_0 = 1$. After absorption of the photon, the electron then falls back to the ground electronic state, which in 10-15% of the time connects to the vibrational continuum [Tielens, 2005]. In this case, the molecule dissociates. Tielens [2005, p. 288] gives the photodissociation rate for H_2 for a plane-parallel, constant density slab, illuminated from one side:

$$k_{\mathrm{UV}}(\mathrm{H_2}) = \beta_{\mathrm{ss}}(\Sigma(\mathrm{H_2}))e^{-\tau_d}k_{\mathrm{UV}}(0)\ [\mathrm{s^{-1}}]. \tag{2.9}$$

Here $k_{\mathrm{UV}}(0)$ is the unshielded photodissociation rate ($\simeq 4 \times 10^{-11} G_0$ s^{-1}), $\Sigma(\mathrm{H_2})$ is the H_2 column density into the cloud, τ_d is the dust optical depth at 1000 Å and β_{ss} is the self-shielding factor. This last factor can be approximated by:

$$\beta_{\mathrm{ss}} = \left(\frac{\Sigma(\mathrm{H}_2)}{\Sigma_0}\right)^{-\frac{3}{4}}, \tag{2.10}$$

where $\Sigma_0 = 10^{14}$ cm^{-2} for the column density range $10^{14} \lesssim \Sigma(\mathrm{H}_2) \lesssim 10^{21}$ cm^{-2}.

For our disk $e^{-\tau_d} \simeq 1$ as the dust content is less than 10^{-3} times the galactic value [Cazaux and Spaans, 2004], and the molecular hydrogen fraction is about 1 in 10^3 particles. Because the disk's total surface density is in the range of $\Sigma = 10^{21} - 10^{23}$ cm^{-2}, $\Sigma(\mathrm{H}_2) = 10^{18} - 10^{20}$ cm^{-2}, which keeps it in the range of applicability for β_{ss}. Modifying the rate equation to get the photodissociation timescale, dependent on the total surface density Σ, gives:

$$t_{\mathrm{pd}} = \frac{1}{k_{\mathrm{UV}}(\mathrm{H}_2)} = \frac{1}{\beta_{\mathrm{ss}} k_{\mathrm{UV}}(0)} \simeq 4.5 \cdot 10^6 \left(\frac{\Sigma}{10^{22}\ \mathrm{cm}^{-2}}\right)^{\frac{3}{4}} \frac{1}{G_0}\ [\mathrm{yr}]. \tag{2.11}$$

The assumption that the gas is illuminated 'from one side' comes from the fact that stars are also formed within the disk. Those stars have a far larger contribution to the background radiation than stars from far outside the disk. If such a star is formed close to where one is looking in the disk, then it outshines everything else and that region is effectively illuminated from one side. See section 4.1 for more elaboration on these stars.

2.4 Shearing time

The gas does not necessarily flow with the same angular speed at every distance from the central black hole. On a scale relatively small to the size of the disk and sufficiently far from the center, the gas flow can be approximated by an infinite straight flow in one spatial direction. To find the time it takes for shear to tear apart a cloud of gas, we can utilize the example of a two-dimensional flow between two parallel plates, where the plates are represented by the 'rings' of gas just outside of the cloud.

With the cloud a size of $2l$, the 'plates' are a distance $2l$ apart and stretch out very far to both sides. The bottom of the cloud has a relative velocity u with respect to the top, which means that there is a velocity gradient between top and bottom, represented by $v(y)$. The flow is only in the direction parallel to the plates; only v_x is non-zero, and constant. This situation is steady-state, as the fluid looks the same at every moment.

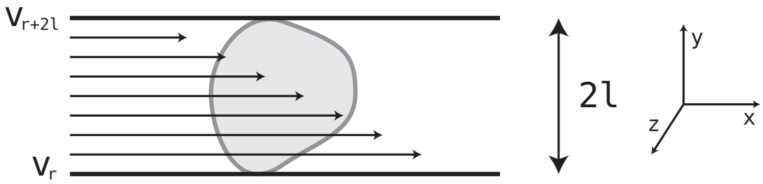

Figure 2.3: Cloud in a velocity field. The $-y$-direction is towards the center.

Is the fluid incompressible? Incompressible fluids have the quality that they are divergence free, $\nabla \cdot \mathbf{v} = 0$, which would enable us to use the Navier-Stokes equation. As we assume that there are no shocks in the gas, we can say that the gas is indeed incompressible.

To estimate the shear time for a given cloud, we first need to find the shear rate. This rate is defined as $\dot{\gamma} = \frac{\partial v}{\partial y}$ $[\frac{\text{cm s}^{-1}}{\text{cm}}]$, where v is the (non-constant) fluid velocity between the plates. See again figure 2.3. This means we actually have to find the velocity difference between the points of the cloud closest to and farthest from the center to know the shear time. Therefore we take the Navier-Stokes equation:

$$\rho \frac{\partial \mathbf{v}}{\partial t} + \rho(\mathbf{v} \cdot \nabla)\mathbf{v} = -\nabla p + \mathbf{f} + \eta \nabla^2 \mathbf{v}, \tag{2.12}$$

where ρ is the gas density, $\mathbf{v}$ the three-dimensional gas velocity, p the pressure, $\mathbf{f}$ is the external body force, and η the viscosity of the fluid. For simplicity, $\eta = 1$. There is no external body force, which means that $\mathbf{f} = 0$. Now we look at the different components. In the z-direction everything is 0, because by assumption there is no velocity or pressure gradient in that direction (the fluid is two-dimensional).

In the y-direction:

$$\begin{aligned}
\rho \frac{\partial \mathbf{v}}{\partial t} &= \rho \frac{\partial v_y}{\partial t} = 0, \\
\rho(\mathbf{v} \cdot \nabla)\mathbf{v} &= \rho(v_x \frac{\partial}{\partial x} + v_y \frac{\partial}{\partial y} + v_z \frac{\partial}{\partial z})v_y = 0, \\
-\nabla p &= -\frac{\partial p}{\partial y}, \\
\nabla^2 \mathbf{v} &= (\frac{\partial^2}{\partial x^2} + \frac{\partial^2}{\partial y^2} + \frac{\partial^2}{\partial z^2})v_y = 0,
\end{aligned}$$

because $v_y = 0$. This means that

$$-\frac{\partial p_y}{\partial y} = 0.$$

And in the x-direction:

$$\begin{aligned}
\rho\frac{\partial \mathbf{v}}{\partial t} &= \rho\frac{\partial v_x}{\partial t} = 0, \\
\rho(\mathbf{v}\cdot\nabla)\mathbf{v} &= \rho(v_x\frac{\partial}{\partial x} + v_y\frac{\partial}{\partial y} + v_z\frac{\partial}{\partial z})v_x = \rho v_y\frac{\partial v_x}{\partial y} = 0, \\
-\nabla p &= -\frac{\partial p}{\partial x} = 0, \\
\nabla^2\mathbf{v} &= (\frac{\partial^2}{\partial x^2} + \frac{\partial^2}{\partial y^2} + \frac{\partial^2}{\partial z^2})v_x = \frac{\partial^2}{\partial y^2}v_x,
\end{aligned}$$

because v_x is constant. This means that:

$$\eta\frac{\partial^2}{\partial y^2}v_x = 0.$$

With the boundary conditions that $v = 0$ at $y = 0$ and $v = u$ at $y = 2l$, we find a linear equation $v = ay + b = \frac{u}{2l}y$. With the shear rate $\dot{\gamma} = \frac{\partial v}{\partial y}$, and

$$u = \sqrt{\frac{GM_{c,(r-l)}}{r-l}} - \sqrt{\frac{GM_{c,(r+l)}}{r+l}}, \tag{2.13}$$

we have the shear time:

$$t_{\text{shear}} = \frac{1}{\dot{\gamma}} = \frac{\partial y}{\partial v} = \frac{2l}{u} = 2l \cdot \left(\sqrt{\frac{GM_{c,(r-l)}}{r-l}} - \sqrt{\frac{GM_{c,(r+l)}}{r+l}}\right)^{-1}. \tag{2.14}$$

In figure 2.4 the gas velocity is plotted against the disk radius. Because the enclosed mass (not counting the black hole) is proportional to the radius, and the disk is about $1/0.006 \simeq 170$ times as heavy as the black hole (following the relation found by Magorrian et al. [1998]), at large distances the velocity difference approaches zero.

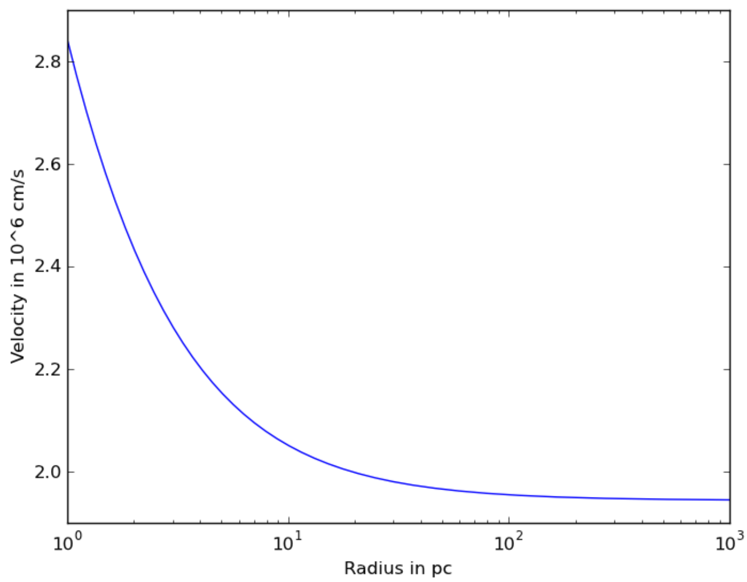

(a)

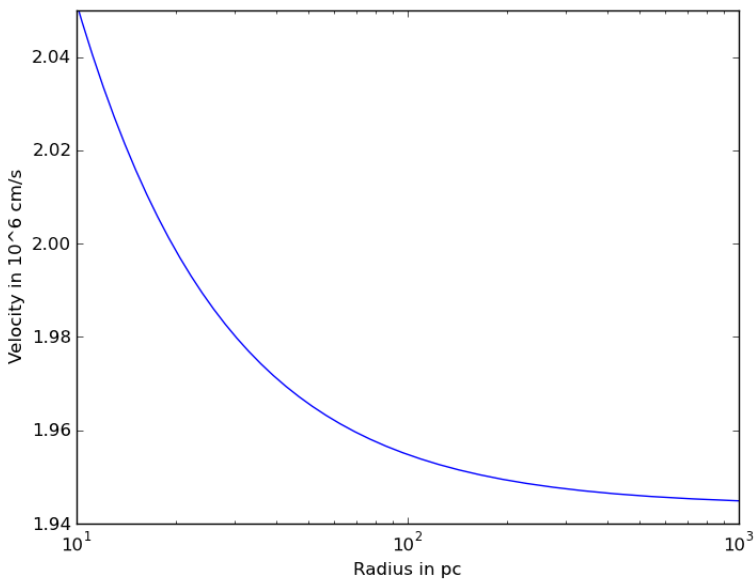

(b)

Figure 2.4: Gas velocities at different radii from the center. Plot (a) shows the whole disk; the central black hole has a distinct influence on the gas velocity in the inner 10 pc. Plot (b) shows radii from 10 pc outwards: the black hole has negligible influence.

Chapter 3

Disk Stability Influences

To assess whether disks are gravitationally stable, one can look at the Toomre stability parameter Q [Ormel, 2008]. Q is defined as

$$Q = \frac{c_g \Omega}{\pi G \Sigma} \approx 4 \cdot 10^{-4} \left(\frac{T}{10^4 \text{ K}} \right)^{\frac{1}{2}} \left(\frac{\Sigma}{10^{22} \text{ cm}^{-2}} \right)^{-1} \left(\frac{r}{100 \text{ pc}} \right)^{-\frac{3}{2}}, \quad (3.1)$$

with c_g the soundspeed, Ω the angular frequency and Σ the surface density. Instability sets in when $Q \lesssim 1$. The numerator gives the stability part in the form of support through pressure (c_g) and through rotation (Ω). The denominator is the instability: $G\Sigma = \frac{GM}{R^2} = a_{\text{grav}}$, the gravitational acceleration.

3.1 Gas collapse

As can be deduced from the Toomre stability parameter, in places with low temperatures, high surface densities and/or far away from the center, the disk becomes (locally) unstable. When instability sets in, the gas can collapse to form bubbles of higher densities than the surrounding medium. These bubbles can eventually form stars, but this will only happen if the disruptive processes remain more efficient than the stabilizing processes. When cooling is the most efficient process in that part of the disk, $t_{\text{cool}} < t_{\text{dyn}}$, the gas can cool fast enough to fragment the gas into smaller bubbles that are the progenitors of stars. When $t_{\text{dyn}} < t_{\text{cool}}$, however, gas cooling cannot keep up with the infall and the temperature will stay high. This means that there is no fragmentation and thus no star formation at that point in the disk. At other points collapse is still possible.

3.2 Star formation

The clouds can be prevented from collapsing if enough disrupting energy from supernovae is injected into the disk. However, it is unknown with what mass distribution the first stars formed, and therefore how many supernovae exploded with what energy at a given time. To understand more of stellar evolution and the star formation history, we can look at the Initial Mass Function (IMF), which quantifies the distribution of masses at birth. Many attempts have been made to find this function (e.g. Salpeter [1955] and Chabrier [2003]) and to find out whether or not a universal IMF exists.

3.2.1 Salpeter IMF

Salpeter [1955] found an empirical expression for the distribution of stars as a function of mass. After several corrections (e.g. Kroupa [2001]) the function is now $\xi(m)\mathrm{d}m \propto m^{-2.35}$, valid for $0.3 \leqslant M_\odot \leqslant 100$, and for the stars currently seen in the Milky Way. This IMF favors small stars over massive stars.

It is likely that for the very early Universe this IMF is not correct, but that a very top-heavy IMF existed [Schneider et al., 2002], as there were no means yet to produce stars with masses much smaller than $30M_\odot$. However, we do not know what this top-heavy function would look like and when exactly it would be valid. We do know that the first objects (Population III) must have produced enough metals to allow a transition from this primordial star formation to the current star formation (Population I/II) [Aykutalp and Spaans, 2011].

3.2.2 PopIII to PopII

The very first stars were likely very massive and short-lived. It is thought that these primordial stars evolved into either supernovae or pair instability supernovae (PISN, which leave no remnant), dependent on their initial mass [Schneider et al., 2002, Heger et al., 2002]. These SNe then enriched the surrounding medium until the IMF changed from top-heavy to Salpeter-like. Wise et al. [2012] state that a single PISN is sufficient to enrich the host halo to a metallicity of $10^{-3}\ Z_\odot$. This metallicity is in the same range as the critical metallicity $Z_{\mathrm{cr}} \simeq 10^{-6} - 10^{-3.5} Z_\odot$ for which the transition to Population II star formation takes place. [Schneider et al., 2002] use a value of $Z_{\mathrm{cr}} \simeq 10^{-4} Z_\odot$ above which atomic cooling is driven by OI, CI and CO line emission for low densities. Dust cooling, however, is already effective for $Z_{\mathrm{cr}} \simeq 10^{-5} Z_\odot$ [Dopcke et al., 2011]. This means that for $10^{-5} \lesssim Z \lesssim 10^{-4} Z_\odot$ dust cooling is already efficient, but metal line cooling is not, so we can ignore the metals. Dust cooling has the advantage over H_2 cooling that it is effective at lower temperatures and higher densities, because it cools by collisions. This mechanism can therefore fragment the larger clouds made by Lyman-α cooling or H_2 cooling.

3.3 Supernova impact

Having established that we can take a Salpeter IMF $\xi(m)\mathrm{d}m = \alpha m^{-2.35}$ for our case, we can deduce how many stars will end as supernovae. Normalizing this function gives $\alpha = 0.266$ and integrating from $8M_\odot$ to $50M_\odot$, the range in which stars end up as supernovae [Heger et al., 2002], we find that about 1.1% of the formed stars do so.

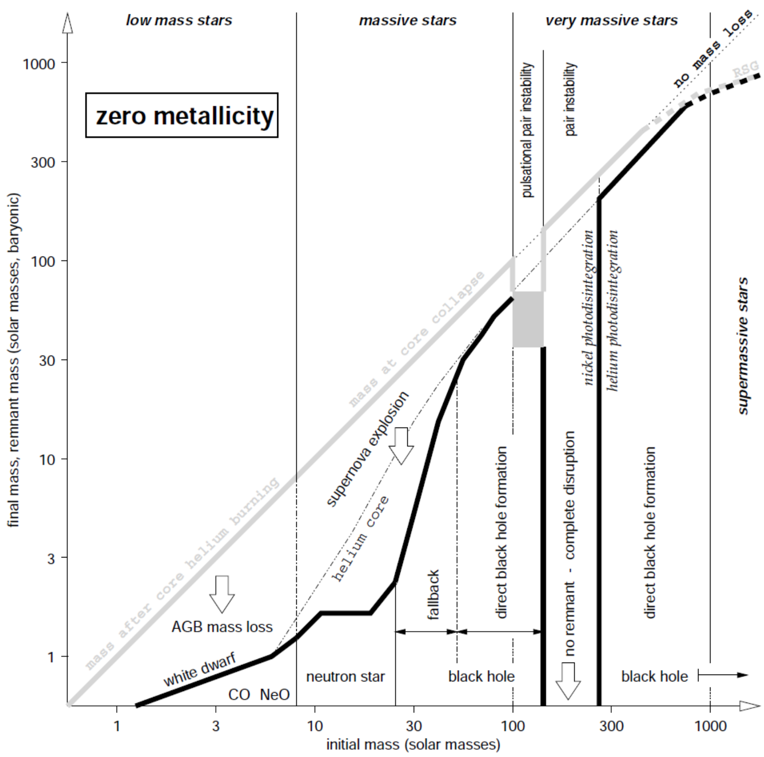

Figure 3.1: The final fate of stars, dependent on mass. Taken from Heger et al. [2002].

Adopting a star formation rate of $0.01M_\odot$ per year, which is roughly equivalent to $1M_\odot$ per year for the Milky Way, we see that there occur $1.1 \cdot 10^{-4}$ SNe per year. The mechanical energy per supernova is $1 \cdot 10^{51}$ erg, of which about 10% is added to the medium as a velocity dispersion increase. Therefore the energy added to the medium per year is $1.1 \cdot 10^{46}$ erg. On average, every particle gets an added velocity of $v = \sqrt{\frac{2E}{m}}$.

Tot calculate the total number of particles in a disk with radius $R = 1$ kpc and a surface density $\Sigma(r) = \frac{10^{24} \cdot 3.086 \cdot 10^{18}}{r}$ cm^{-2}, we use formula 2.1:

$$\int_0^{1\ \mathrm{kpc}} 3.086 \cdot 10^{18} m \frac{10^{24}}{r} 2\pi r \mathrm{d}r = 6.0 \cdot 10^{64}. \tag{3.2}$$

The factor $3.086 \cdot 10^{18}$ is there because r is in cm, not in pc. Now we can find the associated energy per particle per year:

$$E = \frac{\text{total energy}}{\#\ \text{particles}} = \frac{1.2 \cdot 10^{46}}{6.0 \cdot 10^{64}} = 1.8 \cdot 10^{-19}\ \text{erg y}^{-1}. \tag{3.3}$$

This corresponds to a velocity increase of $v = 3.5 \cdot 10^2$ cm s^{-1}, or

$$v = 3.5 \left(\frac{t}{10^6\ \text{yr}} \right)^{\frac{1}{2}}\ \text{km s}^{-1}, \tag{3.4}$$

with $m = 2.92 \cdot 10^{-24}$ g (75% H and 25% He by mass).

To dynamically restructure the disk, an energy $\mathrm{d}U = \frac{GM_{\mathrm{ring}}M_{\mathrm{disk}}}{r}$ is needed, where $M_{\mathrm{ring}} = 2\pi r \Sigma(r) m \mathrm{d}r$ and $M_{\mathrm{disk}} = \int_0^r 2\pi r \Sigma(r) m \mathrm{d}r$. Filling in for $\Sigma(r)$ and m: $M_{\mathrm{disk}} = 5.662 \cdot 10^{19} r$ g and $M_{\mathrm{ring}} = 5.662 \cdot 10^{19}$ dr g. Therefore:

$$U = \int_0^R \frac{GM_{\mathrm{ring}}M_{\mathrm{disk}}}{r} = 6.6 \cdot 10^{53}\ \text{erg}. \tag{3.5}$$

So after $t_{\mathrm{SN}} = 6.6 \cdot 10^7$ yr supernova events will have deposited enough energy in the disk to restructure it. This is with the assumption that every particle in the disk will get exactly as much energy as its neighbor.

Chapter 4

Results, Discussion and Conclusions

A disk with surface density $\Sigma = 10^{23}$ cm^{-2} at $r = 10$ pc and $\Sigma = 10^{21}$ cm^{-2} at $r = 1$ kpc has a total mass $M_{\rm tot} = 8.8 \cdot 10^7 \mathrm{M}_\odot$ (filling in formula 2.1). The central black hole therefore has a mass $M_{\rm BH} = 5 \cdot 10^5$ $\mathrm{M}_\odot$ (following the work of [Magorrian et al., 1998]). This black hole has effect on the gas motion in the inner regions, up to $r \simeq 10$ pc. From there on the enclosed disk mass is much greater than the black hole mass, and the orbital time will not change much.

The orbital time $T_o = \frac{2\pi}{\Omega(r)} \propto r$ is found by filling in formula 2.3 for $\Omega(r)$. At $r = 10$ pc, we find that $T_o = 3 \cdot 10^6$ yr. This is longer than a typical time $t_{\rm dyn} = 7 \cdot 10^5$ yr for a collapsing cloud (formula 2.7). As the orbital time increases with radius, we can conclude that the disk is effectively static on the timescale for collapse from 10 pc outwards.

Can the disk collapse? For that we have to look at Toomre's stability parameter Q, formula 3.1. The disk is unstable where $Q \lesssim 1$. r has the largest influence on Q, so looking at low r will give the largest Q for this disk. Assuming the most stable parameters for Q, which gives Lyman-α cooling at $T = 10^4$ K, $Q = 1.3 \cdot 10^{-3}$ for $r = 10$ pc. This means that the disk is globally unstable, but it is possible to have regions of stability when the temperature is high and the surface density is low. This can for example happen in the region from the center up to 10 pc: if the surface density is around 10^{22} cm^{-2} at 1 pc, the disk becomes marginally stable. For this research, however, it means that we can look for star formation everywhere in the disk from $r = 10$ pc to $r = 1$ kpc.

4.1 H_2 and Lyman-α cooling

The photodissociation timescale (formula 2.11) is dependent not only on the local (surface) density, but also on the local UV background G_0. This UV background can come from other galaxies in the neighborhood, but near stars in the disk it will be completely dominated by the UV radiation emitted by those stars. For H_2 cooling to be important, the H_2 cooling time $t_{\mathrm{cool,H_2}} = 3 \cdot 10^4$ yr should be shorter than the local photodissociation time t_{pd}. What value of G_0 is needed to photodissociate all H_2 molecules in the same time that these cool the medium? Filling in values for 10 pc, 100 pc and 1 kpc, and putting $t_{\mathrm{cool}} = t_{\mathrm{pd}}$, we find that $G_0(10\ \mathrm{pc}) = 8.4 \cdot 10^2$, $G_0(100\ \mathrm{pc}) = 1.5 \cdot 10^2$, and $G_0(1\ \mathrm{kpc}) = 27$. The influence of a PopIII star on its surroundings is quantifiable by approximating it to an O star with a surface temperature of $3.3 \cdot 10^4$ K. Almost all photons emitted by this star are UV photons, so the total UV flux can be approximated by the Stefan-Boltzmann equation $F_* = \sigma T^4 = 6.72 \cdot 10^{13}$ erg cm^{-2} s^{-1}. As $G_0 = 1.6 \cdot 10^{-3}$ erg cm^{-2} s^{-1}, at the surface of this star $F_* = 4.22 \cdot 10^{16} G_0$. We take the radius of this star 10 times the solar radius: $d_* = 2.2 \cdot 10^{-7}$ pc. Then we find the needed G_0 at distance d from the star with:

$$d = d_* \left(\frac{F_*}{G_0} \right)^{\frac{1}{2}} . \tag{4.1}$$

This radius d gives the sphere of influence for this star. Up to d from the star the UV background is high enough to destroy all H_2. In table 4.1 the results are conveniently arranged. Again, this is assuming the UV background from outside the disk is much lower than the flux from the star. From these values we can see that the influence of a star is very local, as the disk would need its own mass in stars to keep up the UV background for the whole disk.

r [pc]	G_0 [erg cm^{-2} s^{-1}]	d [pc]
10	$8.4 \cdot 10^2$	1.6
100	$1.5 \cdot 10^2$	3.7
1000	27	8.8

Table 4.1: The minimum UV background in G_0 needed to prevent H_2 cooling, at different radii from the center of the disk. The distance d is the maximum distance from an O star, with surface temperature $T = 3.3 \cdot 10^4$ K and radius $d_* = 10 R_\odot$, where no H_2 can exist.

4.2 Collapse

Having established that we can look for possible star formation at radii $r = 10$ pc and outwards, we can now try to find the products. Comparing the different timescales t_{dyn}, t_{cool}, t_{pd}, t_{shear} and the time it takes for SNe to dynamically restructure the disk t_{SN}, star formation is only possible when one of these scenarios happen:

1. $t_{\mathrm{cool,\,H_2}} < t_{\mathrm{dyn}} < t_{\mathrm{pd}}$, $t_{\mathrm{dyn}} < t_{\mathrm{shear}}$, and $t_{\mathrm{dyn}} < t_{\mathrm{SN}}$,

2. $t_{\mathrm{cool,Ly}\alpha} < t_{\mathrm{dyn}} < t_{\mathrm{shear}}$, and $t_{\mathrm{dyn}} < t_{\mathrm{SN}}$.

In table 4.2 the results from computations at different radii are listed. The shearing time is computed up to 100 pc, but only for the largest clouds. For smaller clouds and clouds farther from the center this time only gets longer. For reference: $t_{\mathrm{cool,\,H_2}}(200\ \mathrm{K}) = 9 \cdot 10^5$ yr, $t_{\mathrm{cool,\,H_2}}(700\ \mathrm{K}) = 3 \cdot 10^4$ yr, and $t_{\mathrm{cool,Ly}\alpha} = 5 \cdot 10^2$ yr.

Clouds can collapse when the Jeans radius is sufficiently small compared to the disk, i.e. $l = \frac{\lambda_J}{2} \lesssim 10$ pc. Therefore from $r \simeq 200$ pc outwards, the disk will very probably not form any structure. This can also be seen from the fact that $t_{\mathrm{dyn}} \to t_{\mathrm{SN}}$ for large radii. For the region between 10 pc and 50 pc, however, it is very much possible to form stars of a few $10^2 - 10^3 M_{\odot}$, if the UV background is low enough. Near already formed stars only $M_J =$ few $10^4 - 10^5 M_{\odot}$ can collapse, which can directly form black holes (singular collapse). These could be seed black holes [Spaans and Silk, 2006]. The region between 50 pc and 200 pc is another potential hotbed for black holes, with masses of $10^4 - 10^6 M_{\odot}$. If there is still H_2 present, these seeds could, when their density has grown a bit and H_2 cooling becomes effective, fragment into smaller chunks of a few $10^3 M_{\odot}$, potentially forming very massive stars. If there is also enough dust present, the fragments could fragment even further to a few $10^2 M_{\odot}$ stars. Lastly, the central 10 pc will probably not have much star formation, as the densities there ($10^5 - 10^6$ cm^{-3}) are too high for H_2 cooling and the dynamical time is too short for HD or dust cooling. H_2 cooling is not effective above a few 10^4 K, because after the thermalization of the lowest-lying rotational levels in the molecule, cooling becomes less efficient [Bromm and Loeb, 2003]. The central black hole will have too much influence on the surrounding gas to form separate objects. The gas can however be accreted by the black hole. Supernovae can influence the accretion rate, but as $t_{\mathrm{SN}} = 6.6 \cdot 10^7$ yr, which is comparable to an Eddington accretion timescale of 10^8 yr, the accretion is not much hampered.

4.3 Future work

A lot of assumptions have been made during this research. The central object is now taken to be a 'dead' object which does not radiate energy. In reality a $5 \cdot 10^5 M_\odot$ object radiates very much energy up to a few keV. This will alter the physical structure of the disk, as the wings will flare instead of grow linearly, and the radiation from the central object can hit the wings from the side.

Another assumption is that the disk is optically thin for Lyman-α radiation. However, as number densities go up, the disk will become optically thick and cooling becomes inefficient. More information can be found in e.g. Latif et al. [2011].

The metallicity is conveniently chosen between $10^{-6} \lesssim Z \lesssim 10^{-3}$, for which the dust content is negligible in the photodissociation processes and line cooling for metals can still be ignored in clouds, but is high enough to form PopII stars. This is not a stable solution, as every SNe will add more metals to the medium.

Only the initial Jeans mass has been considered. Fragmentation is very much possible for many clouds between 10 pc and 100 pc, but there is no knowing with these approximations what the end result might be. As this topic is still widely studied and no definitive conclusions have been drawn, this is hardly a problem singularly for this research. However, as this is still an open question, it should be noted.

These assumptions limit this research. For an in-depth quantitative analysis, these calculations should be done hydrodynamically and linked to each other. The supernova rate for example will generate negative feedback, for as the disk becomes more 'puffed up', the star formation rate will go down, and in turn less supernovae will form, giving time for the disk to relax again in the potential well. All these kinds of feedback effects are now glossed over.

r [pc]	10	50	70	100	200	500	1000
Σ [cm^{-2}]	$1.0 \cdot 10^{23}$	$2.0 \cdot 10^{22}$	$1.4 \cdot 10^{22}$	$1.0 \cdot 10^{22}$	$5.0 \cdot 10^{21}$	$2.0 \cdot 10^{21}$	$1.0 \cdot 10^{21}$
H [pc]	1	5	7	10	20	50	100
n [cm^{-3}]	$3.2 \cdot 10^{5}$	$1.3 \cdot 10^{3}$	$6.6 \cdot 10^{2}$	$3.2 \cdot 10^{2}$	$8.1 \cdot 10^{1}$	$1.3 \cdot 10^{1}$	$3.2 \cdot 10^{0}$
t_{dyn} [yr]	$1.3 \cdot 10^{5}$	$2.1 \cdot 10^{6}$	$2.8 \cdot 10^{6}$	$4.2 \cdot 10^{6}$	$8.0 \cdot 10^{6}$	$2.0 \cdot 10^{7}$	$4.2 \cdot 10^{7}$
t_{shear} [yr]	$2.3 \cdot 10^{6}$	$4.3 \cdot 10^{7}$	$8.3 \cdot 10^{7}$	$2.1 \cdot 10^{8}$	-	-	-
t_{SN} [yr]	$6.6 \cdot 10^{7}$	$6.6 \cdot 10^{7}$	$6.6 \cdot 10^{7}$	$6.6 \cdot 10^{7}$	$6.6 \cdot 10^{7}$	$6.6 \cdot 10^{7}$	$6.6 \cdot 10^{7}$
M_J [$M_\odot$] (200 K)	-	$1.9 \cdot 10^{3}$	$2.6 \cdot 10^{3}$	$3.7 \cdot 10^{3}$	$7.5 \cdot 10^{3}$	$1.9 \cdot 10^{4}$	$3.8 \cdot 10^{4}$
M_J [$M_\odot$] (700 K)	$7.8 \cdot 10^{2}$	$1.2 \cdot 10^{4}$	$1.7 \cdot 10^{4}$	$2.4 \cdot 10^{4}$	$4.9 \cdot 10^{4}$	$1.2 \cdot 10^{5}$	$2.5 \cdot 10^{5}$
M_J [$M_\odot$] (10^4 K)	$4.2 \cdot 10^{4}$	$6.6 \cdot 10^{5}$	$9.2 \cdot 10^{5}$	$1.3 \cdot 10^{6}$	$2.6 \cdot 10^{6}$	$6.6 \cdot 10^{6}$	$1.3 \cdot 10^{7}$
l [pc] (200 K)	-	$2.0 \cdot 10^{0}$	$2.8 \cdot 10^{0}$	$4.0 \cdot 10^{0}$	$8.0 \cdot 10^{0}$	$2.0 \cdot 10^{1}$	$4.1 \cdot 10^{1}$
l [pc] (700 K)	$2.4 \cdot 10^{-1}$	$3.7 \cdot 10^{0}$	$5.2 \cdot 10^{0}$	$7.4 \cdot 10^{0}$	$1.5 \cdot 10^{1}$	$3.7 \cdot 10^{1}$	$7.6 \cdot 10^{1}$
l [pc] (10^4 K)	$9.0 \cdot 10^{-1}$	$1.4 \cdot 10^{1}$	$2.0 \cdot 10^{1}$	$2.8 \cdot 10^{1}$	$5.6 \cdot 10^{1}$	$1.4 \cdot 10^{2}$	$2.8 \cdot 10^{2}$

Table 4.2: Different quantities at different radii r from the center of the disk: the surface density Σ, the height $H = 0.1 \cdot r$, the number density n, the dynamical time, shearing time, and supernova time $t_{\text{dyn}}, t_{\text{shear}}$, and t_{SN}, and the Jeans masses M_J and Jeans radii $l = \frac{\lambda_J}{2}$ for different cooling mechanisms and temperatures.

Bibliography

A. Aykutalp and M. Spaans. The Complexity that the First Stars Brought to the Universe: Fragility of Metal-enriched Gas in a Radiation Field. *ApJ*, 737:63, August 2011. doi: 10.1088/0004-637X/737/2/63.

R. Barkana and A. Loeb. In the beginning: the first sources of light and the reionization of the universe. *Physics Reports*, 349:125–238, July 2001. doi: 10.1016/S0370-1573(01)00019-9.

M. C. Begelman, M. Volonteri, and M. J. Rees. Formation of supermassive black holes by direct collapse in pre-galactic haloes. *MNRAS*, 370:289–298, July 2006. doi: 10.1111/j.1365-2966.2006.10467.x.

V. Bromm and A. Loeb. The formation of the first low-mass stars from gas with low carbon and oxygen abundances. *Nature*, 425:812–814, October 2003. doi: 10.1038/nature02071.

S. Cazaux and M. Spaans. Molecular Hydrogen Formation on Dust Grains in the High-Redshift Universe. *ApJ*, 611:40–51, August 2004. doi: 10.1086/422087.

G. Chabrier. Galactic Stellar and Substellar Initial Mass Function. *PASP*, 115:763–795, July 2003. doi: 10.1086/376392.

C. J. Clarke and R. F. Carswell. *Principles of Astrophysical Fluid Dynamics*. Cambridge University Press, 1 edition, 2007.

M. Dijkstra, Z. Haiman, M. J. Rees, and D. H. Weinberg. Photoionization Feedback in Low-Mass Galaxies at High Redshift. *ApJ*, 601:666–675, February 2004. doi: 10.1086/380603.

G. Dopcke, S. C. O. Glover, P. C. Clark, and R. S. Klessen. The Effect of Dust Cooling on Low-metallicity Star-forming Clouds. *ApJ*, 729:L3+, March 2011. doi: 10.1088/2041-8205/729/1/L3.

W. F. Frieswijk. *Early stages of clustered star formation -massive dark clouds in throughout the Galaxy-*. Dissertation, 2008.

S. C. O. Glover and T. Abel. Uncertainties in H_2 and HD chemistry and cooling and their role in early structure formation. *MNRAS*, 388:1627–1651, August 2008. doi: 10.1111/j.1365-2966.2008.13224.x.

Q. Guo, S. White, C. Li, and M. Boylan-Kolchin. How do galaxies populate dark matter haloes? *MNRAS*, 404:1111–1120, May 2010. doi: 10.1111/j.1365-2966.2010.16341.x.

Z. Haiman, T. Abel, and M. J. Rees. The Radiative Feedback of the First Cosmological Objects. *ApJ*, 534:11–24, May 2000. doi: 10.1086/308723.

A. Heger, S. Woosley, I. Baraffe, and T. Abel. Evolution and Explosion of Very Massive Primordial Stars. In M. Gilfanov, R. Sunyaev, & E. Churazov, editor, *Lighthouses of the Universe: The Most Luminous Celestial Objects and Their Use for Cosmology*, pages 369–+, 2002.

J. L. Johnson, S. Khochfar, T. H. Greif, and F. Durier. Accretion on to black holes formed by direct collapse. *MNRAS*, 410:919–933, January 2011. doi: 10.1111/j.1365-2966.2010.17491.x.

P. Kroupa. On the variation of the initial mass function. *MNRAS*, 322: 231–246, April 2001. doi: 10.1046/j.1365-8711.2001.04022.x.

M. A. Latif, S. Zaroubi, and M. Spaans. The impact of Lyman α trapping on the formation of primordial objects. *MNRAS*, 411:1659–1670, March 2011. doi: 10.1111/j.1365-2966.2010.17796.x.

J. Magorrian, S. Tremaine, D. Richstone, R. Bender, G. Bower, A. Dressler, S. M. Faber, K. Gebhardt, R. Green, C. Grillmair, J. Kormendy, and T. Lauer. The Demography of Massive Dark Objects in Galaxy Centers. *AJ*, 115:2285–2305, June 1998. doi: 10.1086/300353.

M. Mori and M. Umemura. The evolution of galaxies from primeval irregulars to present-day ellipticals. *Nature*, 440:644–647, March 2006. doi: 10.1038/nature04553.

J. F. Navarro, C. S. Frenk, and S. D. M. White. A Universal Density Profile from Hierarchical Clustering. *ApJ*, 490:493–+, December 1997. doi: 10.1086/304888.

C. W. Ormel. *The early stages of planet formation.* Dissertation, 2008.

E. E. Salpeter. The Luminosity Function and Stellar Evolution. *ApJ*, 121: 161–+, January 1955. doi: 10.1086/145971.

S. Salvadori. *Stellar archaeology: from first stars to dwarf galaxies.* Dissertation, 2009.

D. R. G. Schleicher, M. Spaans, and S. C. O. Glover. Black Hole Formation in Primordial Galaxies: Chemical and Radiative Conditions. *ApJ*, 712: L69–L72, March 2010. doi: 10.1088/2041-8205/712/1/L69.

R. Schneider, A. Ferrara, P. Natarajan, and K. Omukai. First Stars, Very Massive Black Holes, and Metals. *ApJ*, 571:30–39, May 2002. doi: 10.1086/339917.

M. Spaans and J. Silk. Pregalactic Black Hole Formation with an Atomic Hydrogen Equation of State. *ApJ*, 652:902–906, December 2006. doi: 10.1086/508444.

A. G. G. M. Tielens. *The Physics and Chemistry of the Interstellar Medium*. Cambridge University Press, 1 edition, 2005.

D. Whalen, B. van Veelen, B. W. O'Shea, and M. L. Norman. The Destruction of Cosmological Minihalos by Primordial Supernovae. *ApJ*, 682: 49–67, July 2008. doi: 10.1086/589643.

J. H. Wise, M. J. Turk, M. L. Norman, and T. Abel. The Birth of a Galaxy: Primordial Metal Enrichment and Stellar Populations. *ApJ*, 745: 50, January 2012. doi: 10.1088/0004-637X/745/1/50.

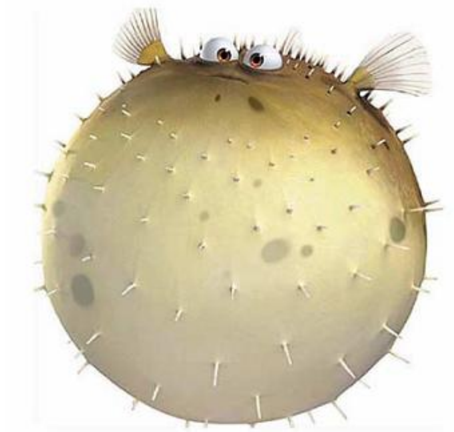

Figure 4.1: A pufferfish. A disk can puff up as well when enough supernovae explode, but it will not puff up *exactly* this way.